



Final Report
Submitted: 31 January 2005

**Wintertime Tethered Balloon Measurements of Meteorological Variables
and Aerosol Characterization in Support of MANE-VU**

Institution: Millersville University, P.O. Box 1002, Millersville, PA 17551

PI: Richard D. Clark
Richard.Clark@millersville.edu
Tel: (717) 872-3930
Fax: (717) 871-2079

Location: 2.4 km WSW of Millersville, PA

Project Timelines:

Preliminary testing through Final Report: 15 Dec 2003 – 2 August 2004

Duration of fieldwork: Six-week period between 1 Jan – 15 Feb 2004

Authorized extension for final report: 31 January 2005

1. PROJECT OVERVIEW

A detailed examination of the structure and evolution of the wintertime boundary layer was conducted from 3 January – 14 February 2004 near Lancaster, PA in support of the research objectives of the Mid-Atlantic/Northeast – Visibility Union. The staging operation was located 2.4 km WSW of Millersville, Pennsylvania; latitude: 39° 59.43' N; longitude: 076° 23.16' W; site elevation: 102 meters MSL.

Two tethered balloons were used to deploy meteorological sensors, condensation particle counters, laser-diode scatterometers, and filter samplers to altitudes of 750 m AGL, while a suite of ground-based instruments measured trace gas and particle concentrations and meteorological parameters, and were used for calibration and intercomparison with balloon-borne instruments. Sensors onboard tethered balloons used in conjunction with surface measurements sampled the wintertime boundary layer with high spatio-temporal resolution, which is essential for the characterization of the coupling between the surface and free atmosphere. Measurements were primarily limited to times when progressive anticyclones moved over the site, bringing clear skies, strong nocturnal radiational cooling, and wind speeds not exceeding the balloon capability of 12 ms⁻¹. These polar air masses influenced the meteorology and chemistry of the site/region for durations ranging from several hours to 2-3 days. This study shows that during these episodes of large-scale subsidence and relatively light winds particulates accumulate in the boundary layer and may deleteriously affect human health.

Studies of the wintertime boundary layer are rare. Much of what we know of the cold season boundary layer comes from studies in the Polar Regions (Parish and Casano 2000; Broeke et al. 2002) and the Grand Canyon (Whiteman et al. 1997). There, the boundary layer forcing and chemistry are very different than that found in the highly populated mid-Atlantic. This study is unique in that it focuses on the structure of the mid-Atlantic wintertime boundary layer and the characterization of particulates in a region influenced by two major urban areas within a 100 km radius, westerly transport from the Ohio River Valley, and local emission sources.

2. DATA COLLECTION

A. Summary of Field Operations

The Millersville University Tethered Atmospheric Boundary Layer System (TABLS) consists of a 12 m³ blimp with a free lift capacity of 7.5 kg, which was used for vertical profiling, and a second 12 m³, oblate spheroid balloon for long-duration time series at constant altitude (Fig. 1). The blimp used for vertical profiling (VP) was limited to wind speeds less than 12-13 ms⁻¹, whereas the spherical balloon used for approximate constant altitude time series (CA) had a free lift capacity of 7.5 kg in calm winds, but gained capacity as a function of increasing wind speed. In all, over 120 vertical profiles were obtained using the

VP and 87 hours were logged on the CA balloon during six notable episodes spanning the six-week project (see Fig. 2).



Fig. 1. Left: Blimp used for vertical profiling (BP); Right: Balloon used for constant altitude time series (CA).

Each balloon platform carried a Väisälä TS111 meteorological sensor package, which recorded and transmitted temperature, pressure, relative humidity, wind speed, and wind direction to a data acquisition system at the surface where it could be displayed and archived. In addition, each ascent/descent vertical profile alternated between carrying an optical scatterometer (TSI DustTrak[®] Model 8520) and a condensation particle counter (TSI Model 3007). The load was too heavy to deploy both instruments simultaneously. A total of 37 DustTrak profiles and 43 CPC profiles were obtained over the six-week project period. A DustTrak was also carried onboard the CA balloon to obtain time series of PM_{2.5} concentrations using laser scatterometry; in all, 87 hours of particle data were obtained. The number of profiles obtained using the BP and the number of hours logged using the CA for each instrument is shown in Fig. 3a.

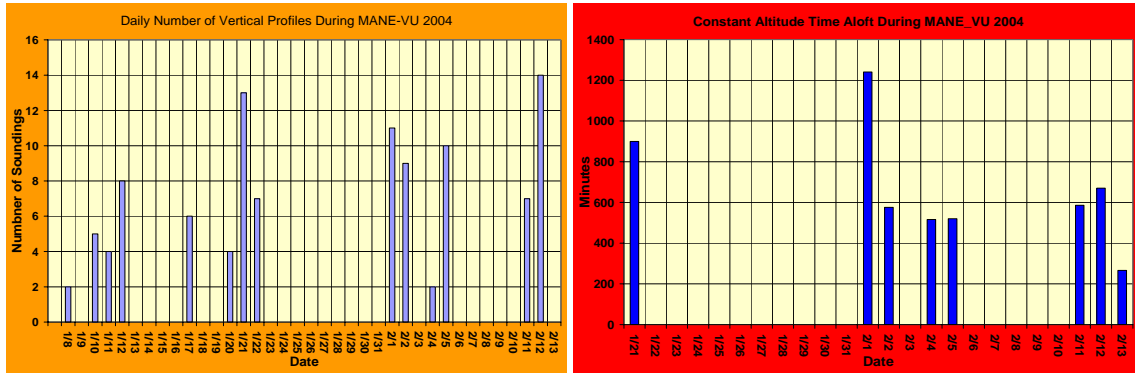


Fig. 2. The daily number of vertical profiles (top) and the daily number of total minutes (bottom) that the two Millersville tethered balloons were deployed.

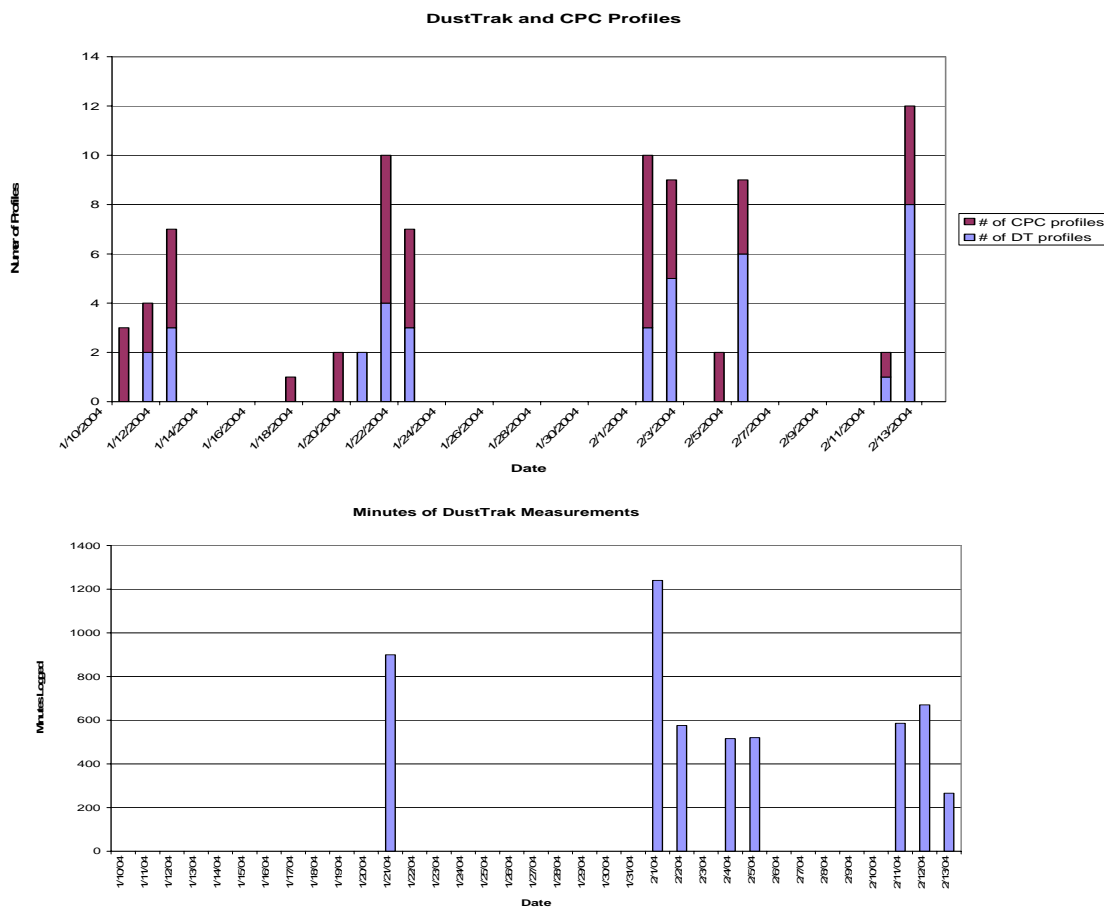


Fig. 3a. The number of DustTrak and CPC profiles obtained with the VP blimp (left), and the number of minutes of time series gathered by the DustTrak onboard the CA balloon for each day they operated.

The CA balloon was also used to deploy an SKC Personal Environmental Monitor for long-duration integrated impaction sampling of particulates with a PM_{2.5} size cut. The time (in minutes) that the PEM collected sample is shown in Fig. 3b. A summary of balloon-borne instrument and specifications is shown in Tables 1 and 2.

PEM-MINUTES SAMPLED

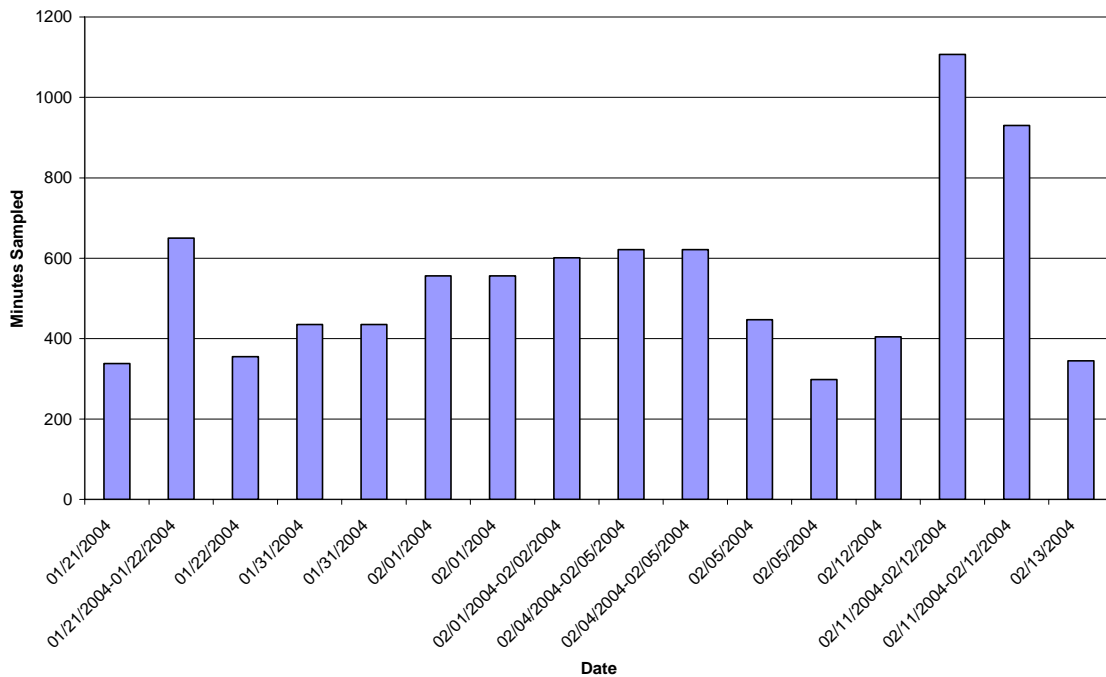


Fig. 3b. The number of minutes logged by the PEM impaction samplers for each day they operated.

Surface instruments included a portable meteorological tower for conventional atmospheric variables, three API trace gas analyzers (NO/NO₂/NO_x, SO₂, and CO), and a TSI 3-wavelength nephelometer (Model 3563) for total and back scattering coefficient (β). Additional instrumentation included a Magee Scientific Aethalometer for BC and UV-C concentrations and a MetOne Model 9012 Ambient Aerosol particle counter, which measured particle concentrations in six size bins ranging from 0.3 μm to greater than 0.8 μm . The Aethalometer and MetOne were on loan from NESCAUM and the University of Maryland, respectively. A summary of surface sensors and specifications is shown in Table 3. In addition to the field instruments, Eta and WRF gridded data, satellite and radar imagery, surface and upper data, EPA PM_{2.5} data, and HYSPLIT trajectories were archived at Millersville University in order to later place the site measurements into a regional context. ***The complete database for the entire project, including aloft data from each balloon, surface data, and archived data has been transferred to NESCAUM in accordance with the contracted deliverables.***

TABLE 1: BLIMP (VP) SENSOR SPECIFICATIONS

Variable or Instrument	Method	Range	Resolution	Response Time	Repeatability	Sampling Frequency
Temperature	Capactive wire	-50 ... + 60 C	0.1 C	0.2 s	0.10 C	1 second
Humidity	Thin film capacitor	0 ... 100%	0.1%	< 0.5 s @ 20 C	2%	1 second
Pressure	Silicon sensor	500 ... 1080 hPa	0.1 hPa	N/A	0.4 hPa	1 second
Wind speed	3-cup anemometer	0 ... 20 m/s	0.1 m/s	N/A	N/A	1 second
Wind direction	Digital compass	0 ... 360 deg	1 deg	N/A	N/A	1 second
PM2.5 Conc (DustTrak Model 8520) Temp range 0 – 50 C (Calibrated for standard ISO 12103-1, A1 test dust)	90 deg Laser-diode photometry Flow Rate 1.7 L/min	0.001 ... 100 mg/m ³	± .1% of reading or 0.001 mg/m ³			10 second thru 1/22/04 1 second after 1/22/04
Condensation Particle Counter (TSI Model 3007) Temp range 0 – 50 C	Cloud chamber w/ optical scatterometer Flow Rate 700 cc/min	0.01 ... 1.0 µm; 0 ... 100,000 cm ⁻³	1 particle cm ⁻³			1 second

TABLE 2: BLIMP (CA) SENSOR SPECIFICATIONS

Variable or Instrument	Method	Range	Resolution	Response Time	Repeatability	Sampling Frequency
PM2.5 Conc (DustTrak) Temp range 0 – 50 C (Calibrated for standard ISO 12103-1, A1 test dust)	90 deg Laser-diode photometry Flow Rate 1.7 L/min	0.001 ... 100 mg/m ³	± .1% of reading or 0.001 mg/m ³	N/A	N/A	1 second thru 2/2/04 3 seconds after 2/2/04
SKC Personal Environmental Monitors for integrated filter samples	Inertial separation/impaction Gravimetric analysis Flow Rate 4 L/min	< 2.5 µm (2.5 µm size cut)	N/A	N/A	N/A	Integrated sample, 4 hours min; 10 hours max.

TABLE 3: SURFACE-BASED INSTRUMENT SPECIFICATIONS

Variable or Instrument	Method	Range	Resolution	Response Time	Repeatability
Temperature	Capactive wire	-50 ... + 60 C	0.1 C	0.2 s	0.10 C
Humidity	Thin film capacitor	0 ... 100%	0.1%	< 0.5 s @ 20 C	2%
Pressure	Silicon sensor	500 ... 1080 hPa	0.1 hPa	N/A	0.4 hPa
Wind speed	3-cup anemometer	0 ... 20 m/s	0.1 m/s	N/A	N/A
Wind direction	Digital compass	0 ... 360 deg	1 deg	N/A	N/A
PM2.5 Conc (DustTrak Model 8520) Temp range 0 – 50 C	90 deg Laser-diode photometry Flow Rate 1.7 L/min	0.001 ... 100 mg/m ³	± .1% of reading or 0.001 mg/m ³		
Condensation Particle Counter (TSI Model 3007) Temp range 0 – 50 C	Cloud chamber w/ optical scatterometer Flow Rate 700 cc/min	0.01 ... 1.0 µm; 0 ... 100,000 cm ⁻³	1 particle cm ⁻³	N/A	N/A
SKC Personal Environmental Monitors for integrated filter samples	Inertial separation/impaction Gravimetric analysis Flow Rate 4 L/min	< 2.5 µm (2.5 µm size cut)	N/A	N/A	N/A
TSI 3-wavelength Nephelometer Model 3563 Scatter-coef of airborne particles	Optical integrating nephelometry: 450 nm (blue), 550 nm (green), 700 nm (red). Flow Rate 20-200 L/min	Sensitivity Blue/green 1.0 x 10 ⁻⁷ m ⁻¹ Red/IR 3.0 x 10 ⁻⁷ m ⁻¹	Drift Less than 2.0x10 ⁻⁷ m ⁻¹ at 30-sec ave time	< 10 sec	
Ozone conc API model 400A	UV absorption EQOA-0992-087	0-100 ppb / 0-10 ppm user selectable	< 0.6 ppb per EPA definition	< 10 sec per EPA definition	N/A
SO ₂ conc API model 100A	Fluorescence EQSA-0990-077	0-50 ppb / 0-20 ppm auto ranging	0.4 ppb RMS	< 20 sec per EPA definition	N/A
NO _x conc API model 200A	Chemiluminescence RFNA-1194-099	0-5 ppb / 0-2000 ppb user selectable	0.4 ppb RMS	< 20 sec per EPA definition	N/A
Magee AE-42 Aethalometer	Dual λ optical Flow Rate: 3.8-4.2 L/min				

B. Quality Assurance Project Plan

Millersville University worked with NESCAUM and R3 EPA to develop a QA project plan prior to the commencement of the field project. All sensors, instruments, and analyzers were calibrated in December 2003 before the field project start date. The field operating procedures are included in the QA plan, which is attached as an Appendix to this document. Mid-project calibrations had to be shelved in part due to the severity of the winter – the 10th coldest on record, and because of the intensity of the work schedule when both balloons were operational. However, routine comparisons were conducted between the balloon-borne instruments and ground-based instruments each time the balloons were retrieved.

C. Staffing and Equipment

The project supervisor (Richard Clark, PI) and 18 undergraduate students were involved in this project. The large number of students was necessary to ensure that no fewer than three personnel were on site during active operations; typically five students were on site at any given time.

D. Field Data Collection

Millersville University was initially contracted to conduct a 30-day project from 3 JAN – 1 FEB 2004. In consultation with NESCAUM (i.e. George Allen), Millersville voluntarily extended this project for an additional 13 days. Millersville University applied for and received FAA waivers allowing balloon operations to continue to an altitude of 750 meters AGL, and fully complied with all FAA restrictions and protocols for the full project duration, including securing an extension from the FAA to continue operations through 15 FEB.

Not much was known or could be gleaned from the manufacturer about the reliability in cold conditions of instruments that were intended for room temperature. This did not present a problem for surface instruments which were contained within a heated trailer. However, aloft instruments had to be “winter-hardened” to ensure that they operated within the range of specified temperatures appropriate to that instrument. To accommodate this requirement, the Millersville group created insulated pockets for each instrument, which were lined with fresh chemically heated pillows just prior to deployment. Before the start of the project, these pillows were tested to ensure that they did not affect particulate concentrations. The temperature of the instrument environment was routinely monitored to ensure that it remained within specification. This procedure worked extremely well, resulting in no data loss even as outside temperatures fell to -4 F at the surface, and -10 F aloft.

E. Data Validation and Report

Millersville University provided data summaries via ftp to George Allen, NESCAUM Project Manager, for each instrument used in data collection during the field project. A summary of the surface instruments that provided continuous measurements is given in Table 4.

TABLE 4: Summary of Ground-based instruments			
Instrument	Variable(s)	Units	Period of measurement
Aethalometer	BC, UV-C	$\mu\text{g}/\text{m}^3$	2 JAN – 13 FEB 2004
TSI 3 λ Model 3563, Neph	Total and back scatter coef.	m^{-1}	8 JAN – 13 FEB 2004
MetOne Model 2010	Particle counts is six size bins	counts/L	7 JAN – 13 FEB 2004
TSI DustTrak Model 8520	PM2.5 estimated from laser scattering	mg/m^3	6 JAN – 13 FEB 2004
TSI CPC Model 3007	Total particle count	$\#/ \text{m}^3$	6 JAN – 13 FEB 2004
API Model 100A SO2 Analyzer	SO2 concentration	ppb	6 JAN – 13 FEB 2004
API Model 200A NO _x Analyzer	NO/NO ₂ /NO _x concentration	ppb	6 JAN – 13 FEB 2004
API Model 300A CO Analyzer	CO concentration	ppm	7 JAN – 13 FEB 2004

Personal Environmental Monitors (SKC type) were deployed at irregular intervals onboard the CA balloon for impaction sampling of PM2.5. The Teflon filters were later sent to HSPH for gravimetric analysis. The PEM data are questionable, either because of poor handling techniques or problems associated with winterizing the pumps.

Each record of measurement was validated by going through the data, line-by-line, searching for illegitimate and systematic errors. Illegitimate records were expunged from the processed data base, although they remain in the raw data archive. An apparent systematic error was identified in the TSI Model 3563 Nephelometer data starting on 8 Jan 2004. Following the field project, this instrument was returned to TSI for calibration and was found to have a bad chopper blade. The submitted data has not yet been corrected for changes in the calibration coefficients, so it should only be used to establish trends, not absolute values for total and back scatter coefficient. We intend to re-run the entire nephelometer data set through a post-processing algorithm, which hopefully will correct this systematic error.

3. PROJECT ACCOMPLISHMENTS

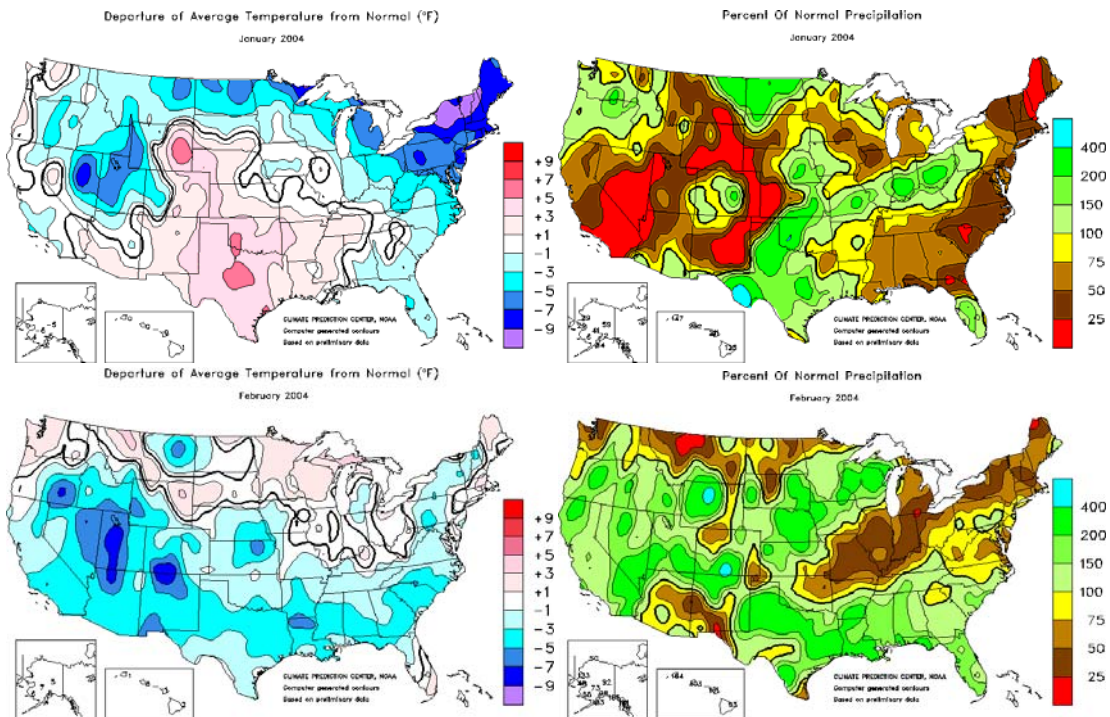
The main scientific objective of the MANE-VU 2004 was to characterize the wintertime boundary layer using dual tethered balloons to document changes in meteorological variables and aerosol concentrations. Millersville compiled a considerable data base of vertical profiles (120) and constant altitude, long-duration, samples (87 hours) of the wintertime boundary layer to an altitude of

750 m AGL, and ground based measurements. This complete data base was ftp'd to NESCAUM for public dissemination.

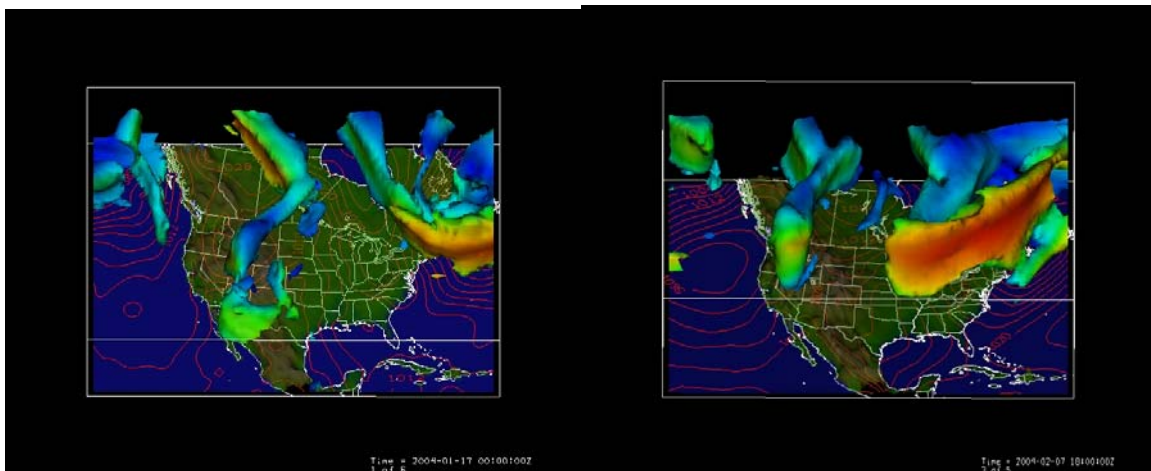
A. Summary Data Analysis

A detailed examination of the structure and evolution of the wintertime boundary layer was conducted from 3 January – 14 February 2004 near Lancaster, PA in support of the research objectives of the Mid-Atlantic/Northeast – Visibility Union (MANE-VU). The Millersville University MANE-VU site was located at a semi-rural, agricultural setting typical of the region at latitude 39° 59.43' N, longitude 076° 23.16' W, and an elevation of 100 m MSL. The site was chosen because of it is representative of the mid-Atlantic piedmont area about halfway distant between the Atlantic coastal plain and the Appalachian Mountains. It has the potential to be affected by four major urban areas: Pittsburgh 300 km to the west, New York City 150 km to the northeast, and Baltimore and Philadelphia with a 100 km radius to the south and east respectively. Lancaster, PA (pop. 50,000) lay 9 km east of the site.

January 2004 was the 10th coldest on record in the mid-Atlantic region with a -6 F departure from normal. The month was also drier than normal with only 30% of normal precipitation. In February 2004, both temperature and precipitation returned to near normal values. However, in the first half of February the temperature was still -2 F below normal and the precipitation was twice normal. For the project period from 3 January - 14 February 2004, the site experienced temperature departures of -6.6 F from normal and 9.6 mm above normal precipitation. The climatological January thaw was absent in 2004 in this area.



The synoptic setting for winter 2004 was dominated by an active pattern of cyclones and anticyclones propagating over the mid-Atlantic region. From 1-27 January, the synoptic pattern has dominated by progressive Rossby waves and embedded short waves transporting frigid air from the Canadian Provinces into the mid-Atlantic, interspersed by periods of zonal flow and a return to near normal temperatures and precipitation. A significant pattern change occurred in late January. The long-wave trough axis shifted to the Midwest and brought relatively warm, moist air into the mid-Atlantic for the remainder of the project. The contrast between the early and later periods is evident in the Eta 500 hPa vorticity—shaded with wind speed shown below.



B. Highlights of Two Cases: 2 FEB and 5-6 FEB 2004

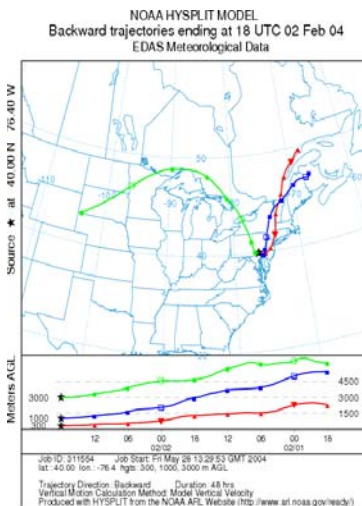
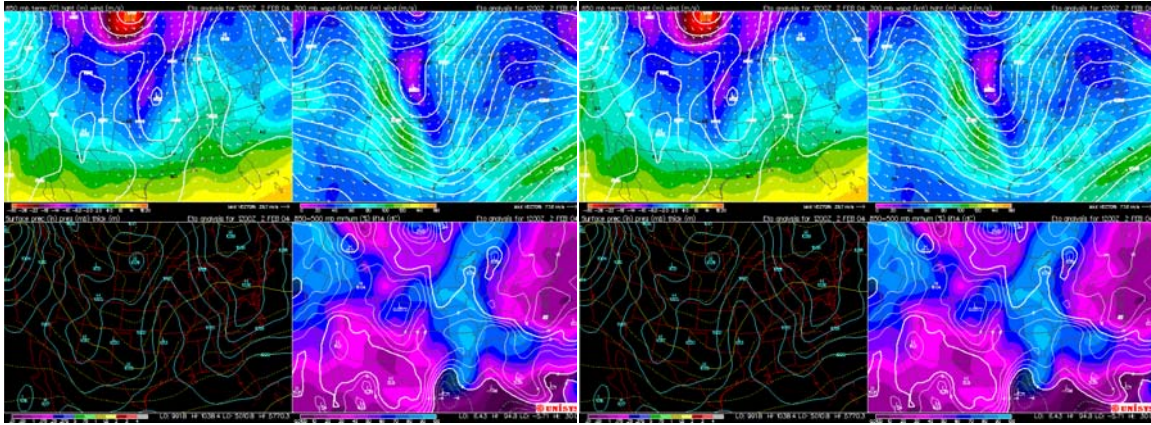
Six case studies were documented between 3 January and 14 February 2004. A feature common to all episodes was the passage of a progressive high pressure system over the study area, and with it the predictable rotation of the wind from a northerly direction to a southerly direction over time.

i. Case Study of 2 FEBRUARY 2004

The 2 February 2004 case study is included as an example of the detailed WBL structure observed during MANE-VU 2004. The period is characterized by a progressive anticyclone through the area and off the coast during the daytime hours. Below is the Eta initialization for 12 UTC 2 Feb and 00 UTC 3 Feb 2004 (below)). NOAA HYSPLIT back trajectories show that air parcels were advected into the region from the north. The model does not capture the decidedly southwesterly flow at the surface, which backed to southeasterly between the surface and 500 m AGL. This backing is evident in the observed vertical wind profile obtained at the site using the blimp.

The first profile of temperature was obtained between 0911-0943 EST when the near-surface layers were experiencing a weak drainage flow over a snow covered surface (the site was at the bottom of a small hill rising to the

southwest). The drainage resulted in mixing of a layer 50 m deep, which weakened the inversion and increased the average deviation of all meteorological variables. This mixing marked the beginning of increases in black carbon concentration, NO_x, and total scattering coefficient that persisted throughout the daytime period.



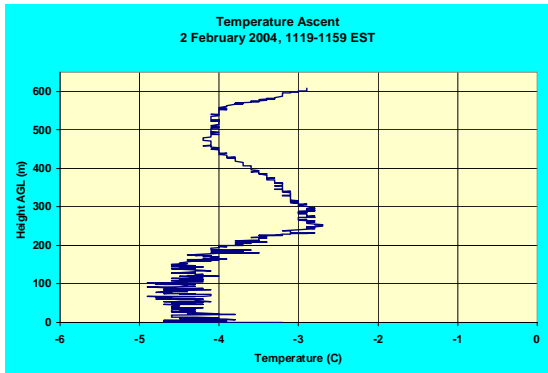
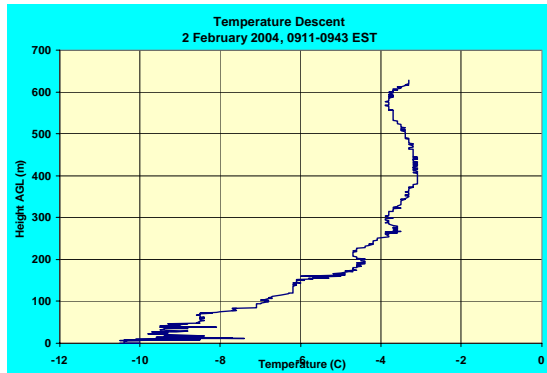
Top Left: Eta initialization for 12 UTC 2 FEB

Top Right: Same except for 00 UTC 3 FEB T

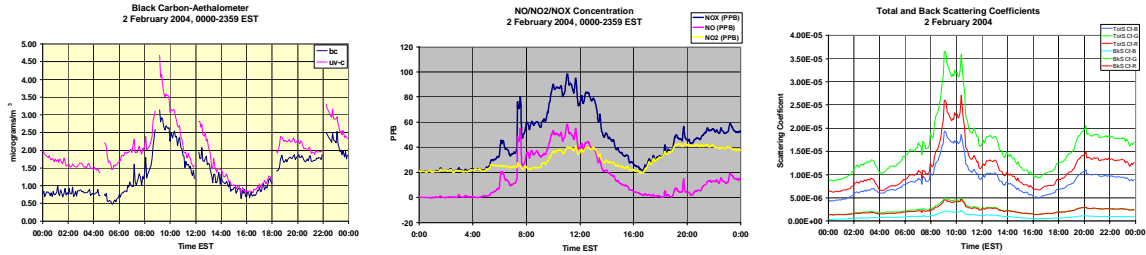
Left: HYSPLIT back trajectories ending 18 UTC 2 FEB;

Below Left: Temperature Profile for 0911-0943 EST;

Below Right: Same except for 1119-1159 EST.

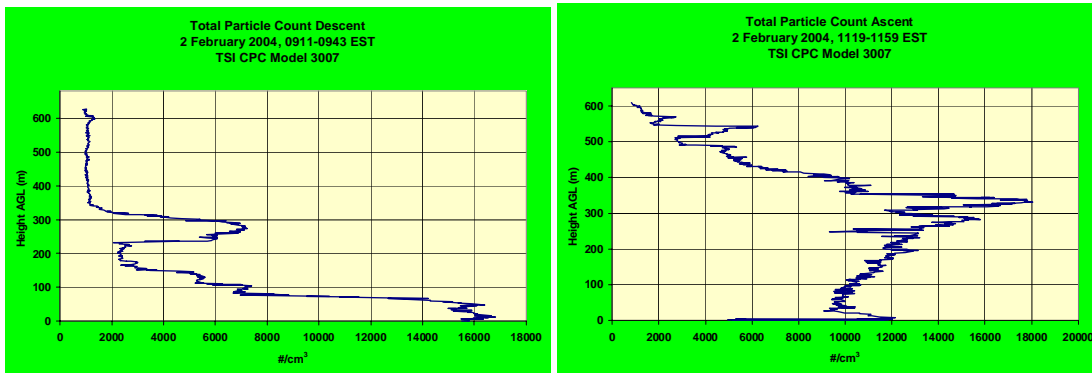


By 1119-1159 EST the encroachment of synoptic gradients had overwhelmed the local drainage and the daytime BL deepened. Air was transported into the region from the southeast (see back trajectory)) as continental polar air mass centered north of the Great Lakes region continued its eastward movement. The depth of the isothermal layer had increased to about 150 m with the remnant inversion remaining largely intact to 250 m AGL.



Above: BC and UC-V, NO/NO₂/NO_x, and total and back scatter coefficients for 2 FEB 2004.

Considerable stratification was also observed in the vertical profiles of total particle count at 0911-0943 and 1119-1159 EST (below). The highest concentrations (16,000 cm⁻³) were observed in the 50 m layer near the surface, and were likely due to local residential burning (i.e., coal furnaces, wood stoves) and drainage into the study area. Above the surface layer, particle counts diminish by a factor of eight in the remnant inversion before increasing again to a local maximum of 7000 cm⁻³ at 270 m AGL. This secondary peak appears to be associated with particles trapped in an aloft inversion. By 1119-1159 EST, the particle count at the surface had decreased from 16,000 to 11,000 cm⁻³, but a notable layer of high particle count was observed residing at the top of the inversion. This feature is embedded in southeasterly flow (3 ms⁻¹ @ 150°) and is probably a combination of both local and regional influences, which also contributed to the elevated amounts of trace gases, scattering coefficient, and black carbon at the surface.

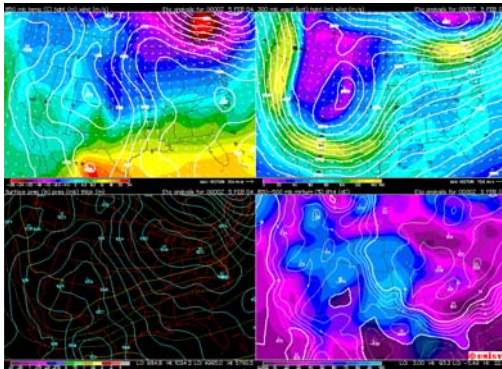


Above: Profiles of total condensation particle count at two hours apart on 2 FEB 2004.

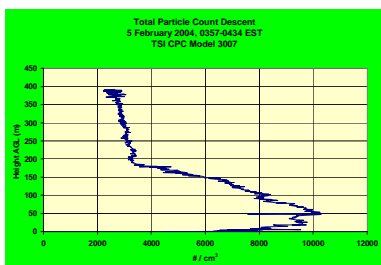
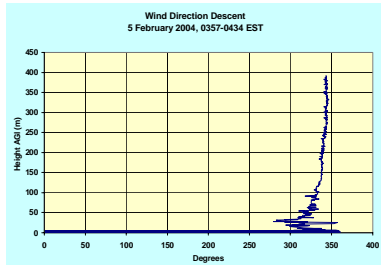
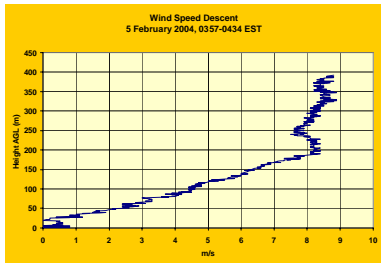
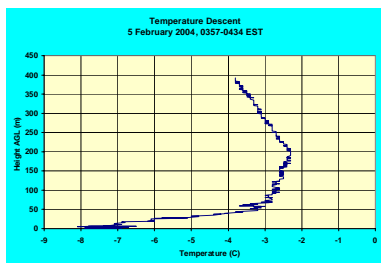
The 2 Feb 2004 case study is characterized by an increase in aerosols and trace gases as an anticyclone moved eastward, which allowed southerly flow to become established in the lowest layers of the WBL. In a cursory way, the 2 Feb case study is reminiscent of summertime cases where the highest concentrations of particulates and traces gases are observed during the daytime period.

ii. Case Study of 5-6 February 2004

The case study of 5 February 2004 is an example of the influence that strong temperature inversions and local emissions sources can have on particulate matter concentrations at night, and is indicative of conditions that occur during when overcast conditions pervade during the daytime period. The overnight period from the 4th to the 5th of February was characterized synoptically by the passage of an extended area of high pressure over the site. Clear sky conditions and strong radiational cooling helped to contribute to the 200 m AGL temperature inversion that persisted until early morning on 5 Feb. Aloft gradients remained strong above the subsidence inversion, with wind speeds exceeding 25 ms⁻¹ at 850 hPa over the site. A 75 ms⁻¹ westerly jet streak was located about 600 km north of the site, with wind speeds on the order of 40 ms⁻¹ at 300 hPa over the site.

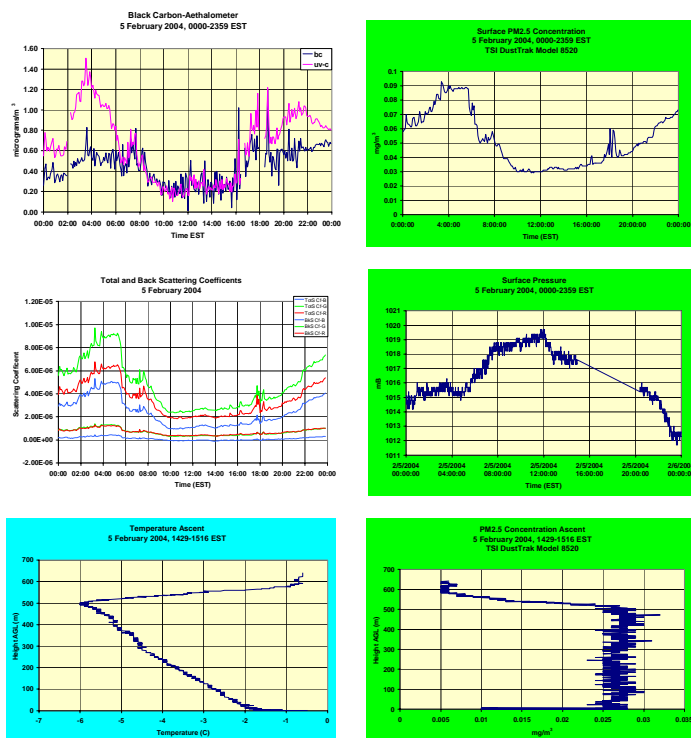


Left: 4-panel Eta initialization for 00 UTC 5 FEB 2004. Clockwise from top left: 950 hPa analysis; 300 hPa wind; surface analysis; and 850-500 hPa relative humidity field



Clockwise from top left: Profiles of temperature, wind speed, wind direction, and total particle count at 0357-0434 EST on 6 FEB 2004.

The strength of the inversion and the shape of the temperature profile had a significant effect on stability and the consequent exchange of momentum in the lower WBL. Winds remained calm in the lowest 25 m AGL, then increase linearly to 8.5 ms^{-1} between the surface and 200 m AGL. The wind direction was relatively constant over the entire depth. Even in the presence of relatively strong shear ($3.8 \times 10^{-2} \text{ s}^{-1}$), the exchange of momentum and scalars was quelled in the near surface layer. This is evidence in the vertical profile of total particle count obtained using a TSI CPC attached to the TASS, which shows that most of the aerosols were confined to the lowest 50 m AGL. The stability in the lowest 50 m led to a build up of surface concentrations of black carbon, PM2.5 and total scattering coefficient at the surface, as shown in figure series below. Given the time of day and the wind direction, the observed concentrations are probably due to local sources. This is supported by the high UV-C concentrations observed in the Aethalometer trace, suggesting that wood smoke is a primary contributor to the non-black, UV-absorbing aromatic organic filterable material. These increases were occurring at a time of surface pressure rises and reached a maximum concentration around 0400 EST, just before a more accelerated rise in surface pressure.



*Clockwise from top left:
 Surface time traces of BC
 and UV-C; PM2.5
 (DustTrak); surface
 pressure; PM2.5 profile
 (DustTrak) for 1429-1516
 EST; same as previous
 except for temperature;
 total and back scatter
 coefficient; for 6 FEB 2004.*

The ridge axis moved over the site at 1200 EST, however by then, the concentrations had already begun to decrease rapidly as the surface wind increased and replaced the near surface air with cleaner, more diluted air from the north. By 1400 EST, the WBL was well mixed with uniform concentrations

(e.g., $\text{PM}_{2.5} \sim 0.025 \text{ mg m}^{-3}$) observed to an altitude of 600 m AGL. The vertical profiles of temperature and $\text{PM}_{2.5}$ concentrations at the right are shown for comparison. The lapse rate by mid-afternoon was approximately adiabatic over the depth of the 500 m layer. The time series above also reveal the contributions to BC/UV-C, $\text{PM}_{2.5}$, and scattering coefficient from morning and afternoon traffic. The secondary peaks around 0800 and 1800 EST are the response to local traffic. The site was located adjacent to a state road that exhibited a traffic density of about two vehicles per minute during times of “high” traffic, and about one vehicle per two minutes during “low” times.

C. Discussion

Four additional case studies were documented but not included in this preliminary dissemination. The two cases presented herein are by no means intended to be an exhaustive account of the complex structure and evolution of the WBL. Instead, they are intended as examples to illustrate the characteristics of the WBL, as well as to elucidate many of the problems associated with the interpretation of WBL structure and evolution. However, several noteworthy features are present in these examples that were observed throughout this winter campaign. The structure of the wintertime boundary layer is replete with detail even in the presence of strong synoptic gradients aloft. At night under conditions of significant radiational cooling such as seen on 5 Feb, strong temperature inversions can form that quell mixing in the lowest layer, and particulate matter concentrations in the 0.01 to 1 micron range can build up in the near surface layer to values exceeding $3 \times 10^4 \text{ cm}^{-3}$, although this is still half of the summertime equivalents under conditions of strong stability. However, the strong stability present at night can be rapidly destroyed in the daytime, even though sun angles are low and solar insolation is typically less than 500 W m^{-2} in January and February. In the presence of strong baroclinicity in winter, mechanical processes in concert with weak surface heating can quickly erode the stable near surface layers and create deep adiabatic layers that drive the exchange of momentum, heat, and particulate concentrations. Whereas buoyancy dominates the forcing terms in the TKE budget in summer, mechanical production is the principal boundary layer forcing term in winter. Upper level gradients in the presence of progressive waves, strong advection, and the replacement of air masses are what characterize the winter condition. In the daytime, the wintertime boundary layer more closely resembles an adiabatic Ekman layer driven by mechanical processes (shear), with a height that is largely determined by the altitude at which the wind achieves geostrophy. In contrast, the summertime boundary layer in the daytime is largely driven by buoyancy, with the PBL height determined by the mean tops of thermals. Most of the baroclinicity in summer is induced at the surface by discontinuities that lead to differential heating and cooling. In particular, the mid-Atlantic region is subject to gradients created by the discontinuities that establish between the coastal plain and the Appalachian Mountains. Certainly, the winter landscape has its share of surface discontinuities (e.g., snow cover, land-ocean contrasts), but the reduced solar

insolation combined with synoptic-scale forcing in the presence of atmospheric waves tend to diminish the establishment of persistent local and regional surface gradients. A further example of this contrast between seasonal boundary layers is the notable lack of the boundary layer-induced low-level jet (LLJ) in winter. On only one occasion was a LLJ observed during this study, and with the lack of upper level wind data above the site, its unequivocal existence could not be confirmed. On the other hand, the LLJ is a recurrent feature of the mid-Atlantic summertime environment formed by differential heating along the Atlantic piedmont (Clark, 2000). The LLJ forms as a complex interaction that involves the near surface gradients that give rise to a pressure gradient force that weakens with height (i.e., most of the summertime baroclinicity is generated near the surface and decreases with height), the sudden cessation of turbulent mixing around sunset, and the ensuing inertial oscillation of the wind field as it attempts to adjust to the mass field. Near surface baroclinicity as a response to differential heating is virtually absent in winter, and what there is can easily be overwhelmed by larger-scale circulations. The LLJs that do exist in winter are a misnomer. In fact, the typical wintertime “LLJ” is a transverse indirect return circulation (Dine’s Compensation) induced through mass continuity in the exit region of an upper tropospheric jet located at a pressure altitude of about 850 hPa. It does not exhibit the classic inertial turning because it is entrained into the flow in a matter of hours.

That the daytime WBL is significantly influenced by larger-scale circulations and is largely mechanically driven should be an advantage for numerical modelers intent on the prediction of particulate matter variability and evolution. On the other hand, the nighttime WBL, with its highly stratified and shallow layering, complex and easily modified structure, and potential for the accumulation of high concentrations of aerosols from local source emissions, will require a deeper understanding of sub-grid scale processes. It has been the goal of this study to elucidate the characteristics of the WBL so as to glean a better understating of these processes.

4. SUMMARY FINDINGS

What these preliminary data show is that the wintertime boundary layer is complex, arguably more so than the summertime boundary layer. While the photochemistry may not be as rich and diverse since reaction rates generally decrease with temperature, several important preliminary conclusions can be drawn from the data:

1. Wintertime boundary layer dynamics, even in the absence of strong baroclinic zones is mechanically driven by shear and, to a lesser extent, radiative forcing;
2. Deep baroclinic layers can exist, and are significantly more frequent than in summer because of the mean position of the polar jet, that completely overwhelm the boundary layer induced forcing. Synoptic, or at minimum

- mesoscale gradients dominate the forcing terms and suppress local and regional circulations;
3. Sustained superadiabatic layers are common in post-cold-frontal conditions due to the complex interaction between snow-covered surfaces and cold air advection aloft. The phase change associated with snowmelt under clear sky conditions after the passage of a cold front with maintain near surface temperatures near 0°C, while cold air aloft increases the lapse rate to adiabatic to superadiabatic levels;
 4. The nocturnal wintertime boundary layer under clear sky, high pressure conditions, exhibits a deep inversion interspersed with multiple shallow layers of strong static stability. These stratified layers are noted for their high aerosol concentrations; in some case five times that of adjacent layer. We believe that these layers trap pollutants emitted in the near-site environment, and probably reflect residential burning of coal and wood. The micro-scale drainage flow that occurs at night is remarkable, with every undulation in topography being a potential source of weak density currents;
 5. Unlike the summer months, the boundary layer nocturnal low-level jet was completely absent in this data. This is not surprising given low wintertime sun angles, uniform often snow covered surfaces or wet exposed surfaces, and strong baroclinic layers that are accompanied by winds increasing with height, all of which work to weaken horizontal near-surface gradients that could give rise to jets.